ON PASSIVE SPOT DAMPING ANOMALIES

by

Dr. Maurice I. Young
Consultant
Vigyan Research Associates, Inc.
Hampton, VA 23666-1325
Telephone: (804) 865-1400

ABSTRACT

Analysis and computation for several damping coupled, lumped parameter models of structural systems demonstrates that passive spot damping treatments become progressively less effective as the natural frequencies of dissimilar modes of vibration coalesce. In the limiting case of dissimilar modes with identical frequencies, an analytical solution is given demonstrating the anomaly of complete loss of damping in one damped mode and the doubling of the damping in another damped mode. These damped modes are shown to be linear combinations of the undamped ones with identical frequencies.

The analysis is extended to continuous structural members such as rectangular membranes and plates, where the anomaly of complete damping loss is again demonstrated. When the aspect ratios of these structural members are selected to yield differing modal patterns with identical natural frequencies, application of passive spot damping yields a pair of damped modes, where one has no damping and the other has twice the effective damping expected.

Finally, a numerical study employing the rectangular plate as an example is presented to quantify the efficacy of a passive spot damping treatment as a function of natural frequency separation. This is then contrasted with the effects of a pervasive damping treatment of the plate.

INTRODUCTION

Vibration control through spot damping treatments can sometimes produce the anomalous result that some of the "damped" modes either remain undamped or have more damping than anticipated. Several lumped parameter examples are presented demonstrating that this is most pronounced when dissimilar modes have the same natural frequency. A plate vibration example is also presented which shows that a spot damping treatment can fail [1,2,3] to damp certain dissimilar modes having the same natural frequency, while others have twice the damping expected. It is shown that frequency matching of damping coupled modes employing spot damping results in nodal and anti-nodal points at the point of application of the spot damping, and that this is the basis of the anomalous result.

ANALYSIS

Consider first two single degree of freedom oscillators of natural frequencies $\omega_1 = (k_1/m_1)^{1/2}$ and $\omega_2 = (k_2/m_2)^{1/2}$. Their displacements x_1 and x_2 are coupled by a dashpot of viscous damping rate c as shown in Figure 1. The coupled equations of motion are

$$m_1\ddot{x}_1 + c(\dot{x}_1 - \dot{x}_2) + k_1x_1 = 0, \tag{1}$$

$$m_2\ddot{x}_2 + c(\dot{x}_2 - \dot{x}_1) + k_2x_2 = 0. \tag{2}$$

Consider now the special case when $\omega_1 = \omega_2 = \omega$. Introducing the relative motion coordinate $y \equiv (x_1 - x_2)$ and the damping fraction $\zeta_1 \equiv (c/2m_1\omega_1)$ and $\zeta_2 \equiv (c/2m_2\omega_2)$, equations (1) and (2) can be combined to yield

$$\ddot{y} + 2(\zeta_1 + \zeta_2)\omega\dot{y} + \omega^2 y = 0. \tag{3}$$

Clearly the modal pattern $x_1 = x_2$ yields no relative motion across the dashpot and the coupled mode has the natural frequency ω and no damping. The modal pattern $x_1 = -x_2$, or $y = 2x_1$ also has the natural frequency ω, but the damping fraction $\zeta = \zeta_1 + \zeta_2$. As a second illustration, consider the damping coupled oscillations of the bouncing and pitching motions of the rigid body shown in Figure 2. The coupled equations of motion are

$$m\ddot{z} + c(\dot{z} + b\dot{\phi}) + kz = 0 \tag{4}$$

$$m\rho^2\ddot{\phi} + cb(b\dot{\phi} + \dot{z}) + ka^2\phi = 0. \tag{5}$$

When the radius of gyration ρ equals the spring offset distance a, the natural frequencies of bouncing and pitching are equal with $\omega = (k/m)^{1/2} = (a/\rho)(k/m)^{1/2}$. Introducing the variable $u \equiv (z + b\phi)$ which is the displacement at the dashpot, equations (4) and (5) can be combined to yield

$$\ddot{u} + 2(\zeta_\phi + \zeta_z)\omega\dot{u} + \omega^2 u = 0 \tag{6}$$

where $\zeta_\phi \equiv (b/\rho)^2(c/2m\omega)$ and $\zeta_z \equiv (c/2m\omega)$. As in the first example, when $u = (z + b\phi)$ is zero, there is an undamped oscillation at natural frequency ω. When $u = (z + b\phi)$ is not zero, the oscillation has the damping fraction $\zeta_u = \zeta_\phi + \zeta_z$. As a third example, consider the three degree of freedom, damping coupled oscillator shown in Figure 3. The three uncoupled natural frequencies are $\omega_u = (k_u/m)^{1/2}$, $\omega_v = (k_v/m)^{1/2}$, and $\omega_\phi = [(k_u d_u^2 + k_v d_v^2)/(m\rho^2)]^{1/2}$. Introducing $\tau \equiv \omega_u t$, $\zeta \equiv (c/2m\omega_u)$ and $' \equiv d()/d\tau$, then the three damping coupled equations of motion in matrix format are

$$\begin{bmatrix} 1 & 0 & 0 \\ 0 & 1 & 0 \\ 0 & 0 & 1 \end{bmatrix} \begin{Bmatrix} u'' \\ v'' \\ \phi'' \end{Bmatrix} + 2\zeta \begin{bmatrix} \sin^2\alpha & \frac{\sin 2\alpha}{2} & \varepsilon \sin\alpha \\ \frac{\sin 2\alpha}{2} & \cos^2\alpha & \varepsilon \cos\alpha \\ \varepsilon \sin\alpha & \varepsilon \cos\alpha & \varepsilon^2 \end{bmatrix} \begin{Bmatrix} u' \\ v' \\ \phi' \end{Bmatrix}$$

$$+ \begin{bmatrix} 1 & 0 & 0 \\ 0 & (\omega_v/\omega_u)^2 & 0 \\ 0 & 0 & (\omega_\phi/\omega_u)^2 \end{bmatrix} \begin{Bmatrix} u \\ v \\ \phi \end{Bmatrix} = \begin{Bmatrix} 0 \\ 0 \\ 0 \end{Bmatrix} \qquad (6)$$

Consider the case of $(\omega_v/\omega_u) = 1$ when the horizontal and vertical motion natural frequencies are equal. The loss of damping anomaly can again be demonstrated: there is a modal pattern $|\bar{u}, \bar{v}, \bar{\phi}|$ corresponding to the pure imaginary eigenvalue $\lambda = j$, $j^2 = -1$. That is, the damping coupled mode occurs at the frequency $\omega = \omega_u$, but with no damping. Direct substitution in equation (6) yields the characteristic determinant

$$\begin{vmatrix} 1 & (2\zeta \cos\alpha)j & (2\zeta\varepsilon) \\ \cos\alpha & \{[(\omega_v/\omega_u)^2 - 1] + (2\zeta \cos^2\alpha)j\} & (2\zeta\varepsilon \cos\alpha)j \\ \varepsilon & (2\zeta\varepsilon \cos\alpha)j & \{[(\omega_\phi/\omega_u)^2 - 1] + (2\zeta\varepsilon^2)j\} \end{vmatrix} = 0 \qquad (7)$$

Expanding and taking $(\omega_v/\omega_u)^2 = 1$, the determinant vanishes for $(\omega_\phi/\omega_u)^2 \neq 1$; the determinant also vanishes for $(\omega_\phi/\omega_u)^2 = 1$ and $(\omega_v/\omega_u)^2 \neq 1$. It does not vanish unless two of the three natural frequencies are equal.

As a final illustration of the spot damping anomaly, consider a simply supported, uniform rectangular plate as illustrated in Figure 4. A dashpot applies a concentrated damping force at the interior point $(\tilde{x},\tilde{y})$. The governing partial differential equation for free vibration follows, where D is the plate flexural rigidity, μ is the plate mass per unit area and d is the viscous damping constant per unit area for the dashpot at $(\tilde{x},\tilde{y})$.

$$D\nabla^4 W(x,y,t) + \mu\ddot{W}(x,y,t) + d\dot{W}(\tilde{x},\tilde{y},t) = 0. \qquad (8)$$

The undamped modal patterns and associated natural frequencies for the integers m and n, and for a plate aspect ratio $N = (a/b)$ are

$$\bar{W}_{mn}(x,y) = \sin(m\pi x/a) \sin(n\pi y/b) \qquad (9)$$

$$\omega_{mn}^2 = (\pi/a)^4 (m^2 + N^2 n^2)^2 (D/\mu) \tag{10}$$

Now consider the case where the differing modal patterns $\overline{W}_{mn}$ and $\overline{W}_{rs}$ have the same natural frequency. Then the plate aspect ratio N is related to the modal integers m, n, r and s by

$$N = [(r^2 - m^2)/(n^2 - s^2)]^{1/2} \tag{11}$$

Now consider the hypothesis that two of the damping coupled modes are

$$\overline{W}_{(+\nu)}(x,y) = \overline{W}_{mn}(x,y) + \nu\overline{W}_{rs}(x,y) \tag{12}$$

$$\overline{W}_{(-\nu)}(x,y) = \overline{W}_{mn}(x,y) - \nu\overline{W}_{rs}(x,y). \tag{13}$$

This hypothesis leads to the eigenvalue equation in λ

$$D\nabla^4[\overline{W}_{mn}(x,y) \pm \nu\overline{W}_{rs}(x,y)] + \mu\lambda^2[\overline{W}_{mn}(x,y) \pm \nu\overline{W}_{rs}(x,y)]$$

$$+ d\lambda[\overline{W}_{mn}(\tilde{x},\tilde{y}) \pm \nu\overline{W}_{rs}(\tilde{x},\tilde{y})] = 0. \tag{14}$$

Taking the parameter $\nu = [\overline{W}_{mn}(\tilde{x},\tilde{y})/\overline{W}_{rs}(\tilde{x},\tilde{y})]$ constrains the displacement at the dashpot location $(\tilde{x},\tilde{y})$ to be either an anti-node or a node point. In the case of an anti-node, the modal pattern

$$\overline{W}_{(+\nu)} = \{\overline{W}_{mn}(x,y) + [\overline{W}_{mn}(\tilde{x},\tilde{y})/\overline{W}_{rs}(\tilde{x},\tilde{y})]\overline{W}_{rs}(x,y)\} \tag{15}$$

has twice the effective damping constant since

$$\overline{W}_{mn}(\tilde{x},\tilde{y}) + \nu\overline{W}_{rs}(\tilde{x},\tilde{y}) = 2\overline{W}_{mn}(\tilde{x},\tilde{y}) \tag{16}$$

and $\overline{W}_{mn}(x,y)$ and $\overline{W}_{rs}(x,y)$ are mutually orthogonal functions despite their matching natural frequencies. This can be seen by multiplying equation (14) by $\overline{W}_{mn}(x,y)$ and integrating over the surface area of the plate. Noting that

$$D\nabla^4 \overline{W}_{mn}(x,y) = \mu\omega_{mn}^2 \overline{W}_{mn}(x,y) \tag{17}$$

the surface integration yields

$$\lambda_{(+\nu)}^2 + [(8d/\mu)\overline{W}_{mn}^2(\tilde{x},\tilde{y})]\lambda_{(+\nu)} + \omega_{mn}^2 = 0 \tag{18}$$

and

$$\zeta_{\substack{\text{effective} \\ (+\nu)}} = \{4(d/\mu)[\overline{W}_{mn}^2(\tilde{x},\tilde{y})/\omega_{mn}]\} \tag{19}$$

which is double that for $\overline{W}_{mn}(x,y)$ when the frequency for $\overline{W}_{rs}(x,y)$ does not match.

In the case of a nodal point at $(\tilde{x},\tilde{y})$, [4,5,6], $W_{(-\nu)} = \{W_{mn}(x,y) - [\overline{W}_{mn}(\tilde{x},\tilde{y})/\overline{W}_{rs}(\tilde{x},\tilde{y})]\overline{W}_{rs}(x,y)\}$ and $\lambda_{(-\nu)}^2 = -\omega_{mn}^2$, the modal pattern occurs with no damping.

It has been demonstrated that spot damping treatments can fail when dissimilar modes have the same natural frequency. A numerical analysis is now presented which reveals that as the natural frequencies of a rectangular plate depart from the normal spacing of dissimilar modes and coalesce, a progressive deterioration of the effective damping provided by spot damping treatments results.

PLATE NUMERICAL ANALYSIS

The governing partial differential equation for the plate is given in equation (8). A modal expansion of undamped modes is employed. That is taking

$$w(x,y,t) = \sum_{m,n=1}^{\infty} \bar{w}_{mn}(x,y)e^{\lambda t} \tag{20}$$

and employing the orthogonality relationships that

$$\int_0^b \int_0^a \bar{w}_{mn}(x,y)\bar{w}_{rs}(x,y)dxdy = 0 \tag{21}$$

for differing integer subscripts and

$$\int_0^b \int_0^a \bar{w}_{mn}^2(x,y)dxdy = \left(\frac{ab}{4}\right). \tag{22}$$

Truncating the modal expansion at N terms, the first N modes of undamped plate vibrations are damping coupled. Employing matrix notation with the generalized coordinates $q_1(t),q_2(t),\cdots,q_N(t)$, the governing matrix differential equation is as follows:

$$\begin{bmatrix} 1 & 0 & \cdots & 0 \\ 0 & 1 & \cdots & 0 \\ \vdots & \vdots & \ddots & \vdots \\ 0 & 0 & \cdots & 1 \end{bmatrix} \begin{Bmatrix} \ddot{q}_1 \\ \ddot{q}_2 \\ \vdots \\ \ddot{q}_N \end{Bmatrix} + \begin{bmatrix} d_{11} & d_{12} & \cdots & d_{1N} \\ d_{21} & d_{22} & \cdots & d_{2N} \\ \vdots & \vdots & \ddots & \vdots \\ d_{N1} & d_{N2} & \cdots & d_{NN} \end{bmatrix} \begin{Bmatrix} \dot{q}_1 \\ \dot{q}_2 \\ \vdots \\ \dot{q}_N \end{Bmatrix}$$

$$+ \begin{bmatrix} \omega_1^2 & 0 & \cdots & 0 \\ 0 & \omega_2^2 & \cdots & 0 \\ \vdots & \vdots & \ddots & \vdots \\ 0 & 0 & \cdots & \omega_N^2 \end{bmatrix} \begin{Bmatrix} q_1 \\ q_2 \\ \vdots \\ q_N \end{Bmatrix} = \begin{Bmatrix} 0 \\ 0 \\ \vdots \\ 0 \end{Bmatrix} \tag{23}$$

where $\omega_1^2, \omega_2^2, \cdots, \omega_N^2$ are the undamped natural frequencies of the undamped plate corresponding to the rectangular plate modal patterns; they are arranged in ascending order of frequency; the damping matrix is symmetrical with

$$d_{ij} \equiv d_{mn,rs} \equiv \left(\frac{c}{ab}\right) \frac{\int_0^b \int_0^a \bar{w}_{mn}(\tilde{x},\tilde{y})\bar{w}_{rs}(\tilde{x},\tilde{y})dxdy}{\mu \int_0^b \int_0^a \bar{w}_{mn}^2(x,y)dxdy}, \tag{24}$$

or

$$d_{ij} \equiv d_{mn,rs} \equiv \left[\frac{4c}{(ab)^2}\right] \bar{w}_{mn}(\tilde{x},\tilde{y})\bar{w}_{rs}(\tilde{x},\tilde{y}). \tag{25}$$

Introducing dimensionless time $\tau \equiv \omega_1 t$ and the reduced damping matrix entries $2\delta_{ij} \equiv (d_{ij}/\omega_1)$, the governing matrix differential equation becomes

$$\begin{bmatrix} 1 & 0 & \cdots & 0 \\ 0 & 1 & \cdots & 0 \\ \vdots & \vdots & \ddots & \vdots \\ 0 & 0 & \cdots & 1 \end{bmatrix} \begin{Bmatrix} q_1'' \\ q_2'' \\ \vdots \\ q_N'' \end{Bmatrix} + 2\begin{bmatrix} \delta_{11}\delta_{12} & \cdots & \delta_{1N} \\ \delta_{12}\delta_{22} & \cdots & \delta_{2N} \\ \vdots & \ddots & \\ \delta_{1N}\delta_{2N} & \cdots & \delta_{NN} \end{bmatrix} \begin{Bmatrix} q_1' \\ q_2' \\ \vdots \\ q_N' \end{Bmatrix}$$

$$+ \begin{bmatrix} (\omega_1/\omega_1)^2 & 0 & \cdots & 0 \\ 0 & (\omega_2/\omega_1)^2 & \cdots & 0 \\ \vdots & \vdots & \ddots & \vdots \\ 0 & 0 & \cdots & (\omega_N/\omega_1)^2 \end{bmatrix} \begin{Bmatrix} q_1 \\ q_2 \\ \vdots \\ q_N \end{Bmatrix} = \begin{Bmatrix} 0 \\ 0 \\ \vdots \\ 0 \end{Bmatrix} \tag{26}$$

A solution is sought in the form

$$\{q(t)\} = \{\bar{q}\}e^{\nu\tau} \tag{27}$$

where

$$\nu \equiv (\lambda/\omega_1) \tag{28}$$

Taking

$$(\omega_p/\omega_1)^2 = \eta_p^2, \qquad p = 1,2,\cdots,N \tag{29}$$

the characteristic determinant follows as

$$\begin{vmatrix} \nu^2 + 2\delta_{11}\nu + \eta_1^2 & 2\delta_{12}\nu & \cdots & 2\delta_{1N}\nu \\ 2\delta_{12}\nu & \nu^2 + 2\delta_{22}\nu + \eta_2^2 & \cdots & 2\delta_{2N}\nu \\ \vdots & \vdots & \ddots & \vdots \\ 2\delta_{1N}\nu & 2\delta_{2N}\nu & \cdots & \nu^2 + 2\delta_{NN}\nu + \eta_N^2 \end{vmatrix} = 0 \qquad (30)$$

The influence of natural frequency separation is now evaluated by systematically perturbing the plate aspect ratio N while preserving the plate area, with mass per unit area and flexural rigidity properties constant, with spot damping coupling the first nine modes. Since the reference aspect ratio N_o has yielded a frequency match and a complete loss of damping, a tabular relationship is now obtained which shows the influence of natural frequency proximity on the effective or virtual damping. This is shown below in Figure 5 in tabular format for several nominal damping levels ranging from 5% to 50% of critical in the fundamental plate mode, with the frequency match occurring in the fourth and fifth modes. It is seen that the loss of damping is almost complete over a significant range of frequencies above and below the match.

PLATE WITH PERVASIVE DAMPING

To contrast the foregoing spot damping case, now consider a uniform, simply supported rectangular plate with uniform or pervasive damping over its entire surface. The governing partial differential equation with equivalent viscous damping per unit area $d_o \equiv \left(\frac{c_o}{ab}\right)$ follows:

$$D\nabla^4 W(x,y,t) + \mu\ddot{W}(x,y,t) + d_o\dot{W}(x,y,t) = 0. \qquad (31)$$

Seeking the solution in the form

$$W(x,y,t) = \hat{W}(x,y)e^{\lambda t} \qquad (32)$$

$$D\nabla^4\hat{W}(x,y) + (\mu\lambda^2 + d_o\lambda)\hat{W}(x,y) = 0 \qquad (33)$$

Since

$$D\nabla^4\overline{W}_{mn}(x,y) = \mu\omega_{mn}^2\overline{W}_{mn}(x,y) \qquad (34)$$

for $d_o = 0$, the undamped case, it follows that the undamped modal functions also are solutions for the case of pervasive damping with the characteristic equation

$$\mu\lambda^2 + d_o\lambda + \mu\omega_{mn}^2 = 0, \qquad (35)$$

or

$$\left(\frac{\lambda}{\omega_{mn}}\right)^2 + \left(\frac{d_o/\mu}{\omega_{mn}}\right)\left(\frac{\lambda}{\omega_{mn}}\right) + 1 = 0. \qquad (36)$$

Since the effective pervasive viscous damping ratio for mode mn is given by

$$\zeta_{mn}\omega_{mn} = \left(\frac{d_o}{2\mu}\right), \tag{37}$$

a direct comparison of spot damping and pervasive damping can now be inferred. It is seen that barring frequency matching in the case of spot damping

$$\zeta_{mn}\omega_{mn} = \left(\frac{d}{2\mu}\right) \bar{W}_{mn}^2(\tilde{x},\tilde{y}). \tag{38}$$

Since $\bar{W}_{mn}^2(\tilde{x},\tilde{y})$ varies from zero to unity, the spot damping level per unit are required exceeds the pervasive damping level in the ratio

$$\left(\frac{d}{d_o}\right) = \bar{W}_{mn}^{-2}(\tilde{x},\tilde{y}), \tag{39}$$

providing that no two natural frequencies coalesce. Factoring in the influence of the distributed or pervasive damping over the entire plate area A = ab, the equivalent effective spot damping level follows as

$$d = d_o(ab)\bar{W}_{mn}^{-2}(\tilde{x},\tilde{y}) \tag{40}$$

to achieve the same fraction of critical damping in the mn-th mode.

CONCLUSION

Passive spot damping treatments are seen to be straightforward in concept, but potentially ineffective when neighboring, but differing modal patterns have natural frequencies that are close to one another. In the special case of matching natural frequencies the effective damping fraction is zero. This stems from the appearance of a nodal point at the spot damping point of application. In fact, the unusual nodal patterns [5] when frequency matches occur can render broader spot and localized damping treatments ineffectual also. Nevertheless, spot damping treatments are attractive in their simplicity compared to pervasive ones, providing true anti-nodal points of application can be found. This is difficult when frequency matches exist.

Acknowledgment

This research is supported by the National Aeronautics and Space Administration, Langley Research Center under NASA Contract No. NAS1-18585. The computations for plate damping in the table were provided by Dr. Raymond G. Kvaternik of NASA Langley Research Center, Structural Dynamics Division, Configuration Aeroelasticity Branch.

REFERENCES

[1] P. H. Geiger 1953 *Noise Reduction Manual*. University of Michigan Engineering Research Institute.

[2] D.I.G. Jones 1967 *Shock and Vibration Bulletin*, 36 (4), 9-24. Damping of Structures by Viscoelastic Links.

[3] M. I. Young 1989 *Journal of Sound and Vibration*. In press. Spot Damping Anomalies.

[4] R. Courant and D. Hilbert 1953 John Wiley and Sons, Inc. (301-302) *Methods of Mathematical Physics*.

[5] F. Pockels 1891 B. G. Teubner (76-85) *Uber Die Partielle Differentialgleichung* $\Delta u + k^2 u = 0$.

[6] S. H. Crandall 1956 McGraw-Hill Book Co., Inc. (76-77) *Engineering Analysis: A Survey of Numerical Procedures*.

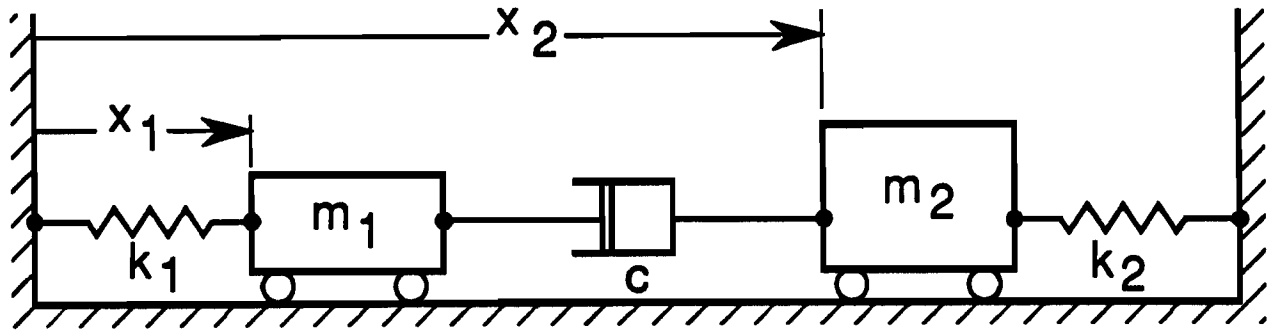

Figure 1. Dashpot Coupled System with Two Degrees of Freedom.

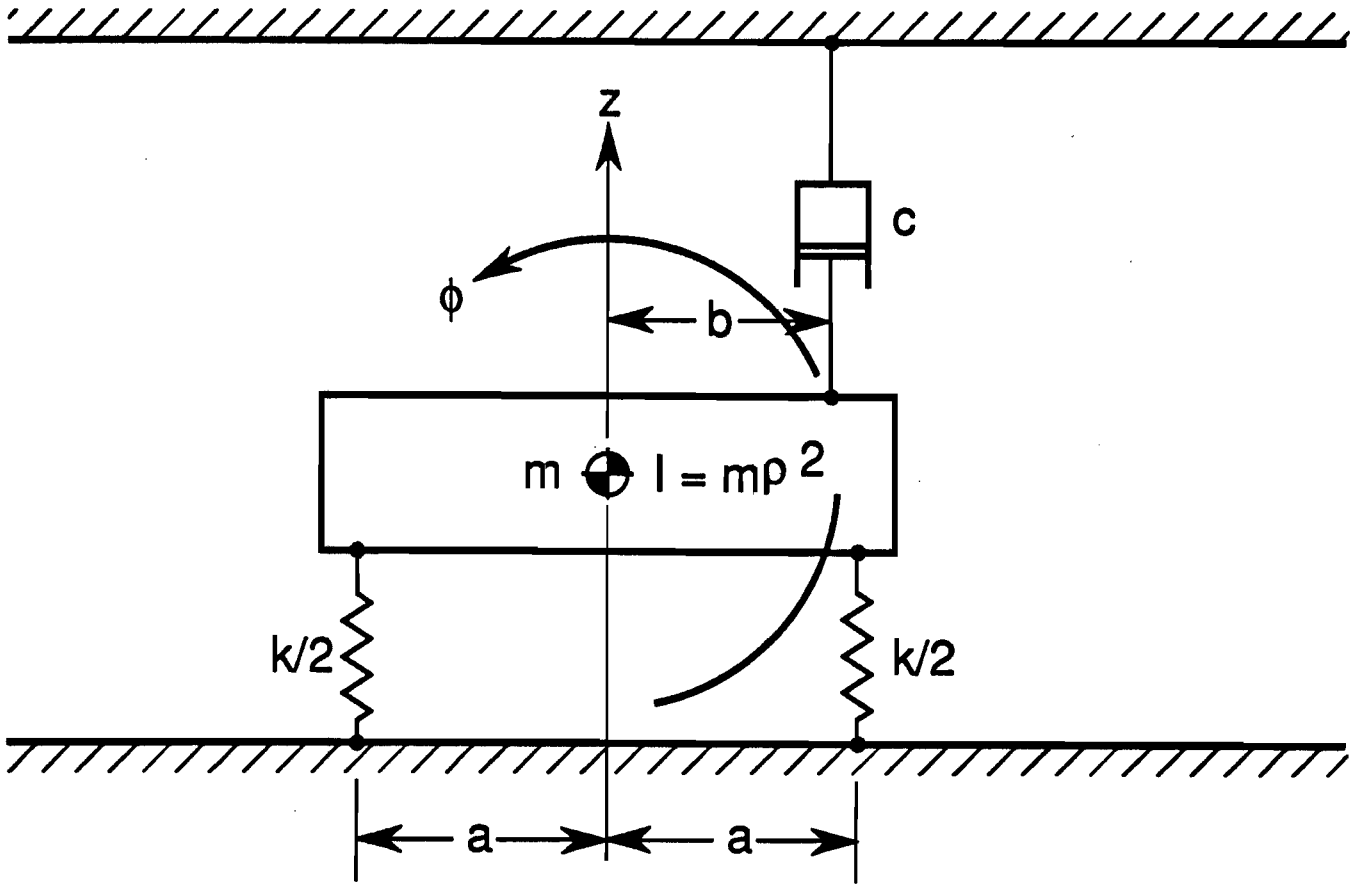

Figure 2. Dashpot Coupled System with Bounce and Pitch Freedoms.

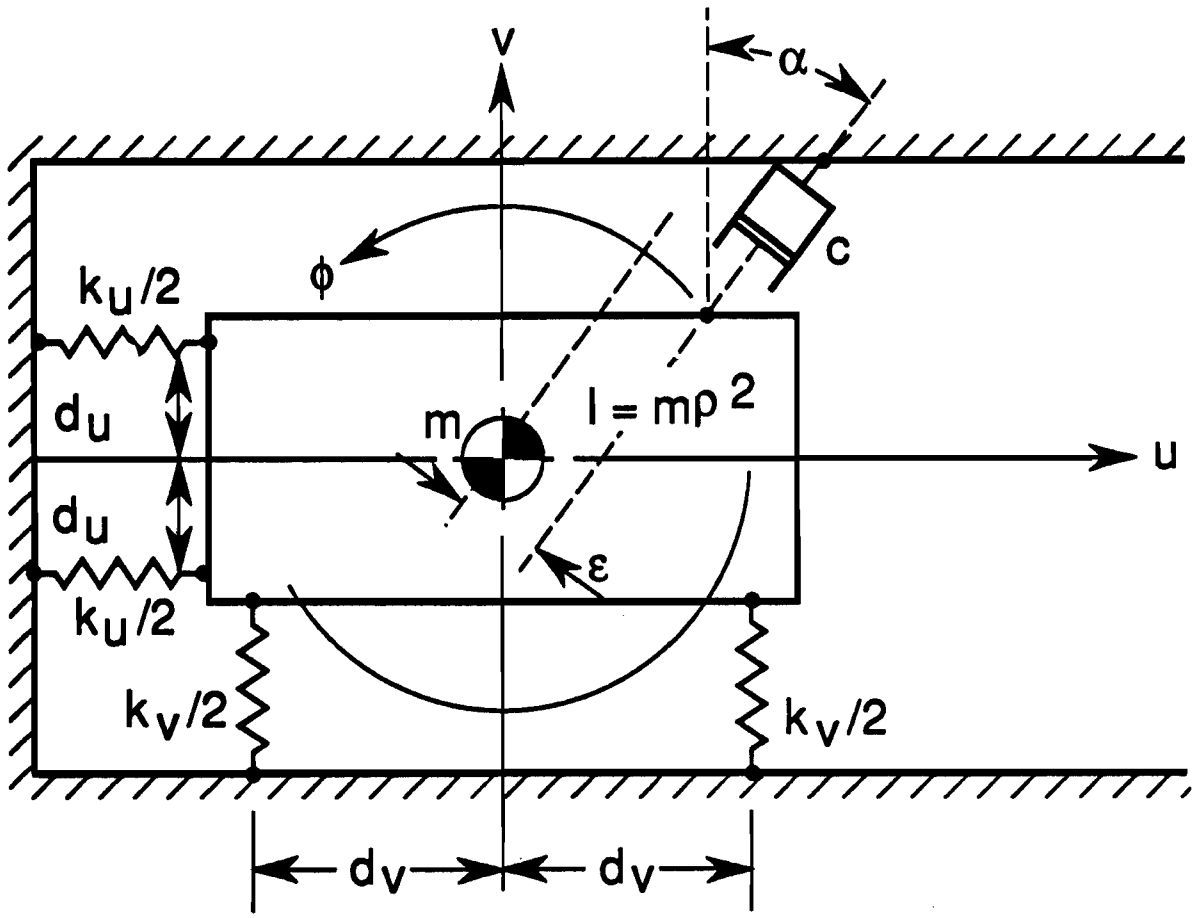

Figure 3. Dashpot Coupled System with Three Degrees of Freedom.

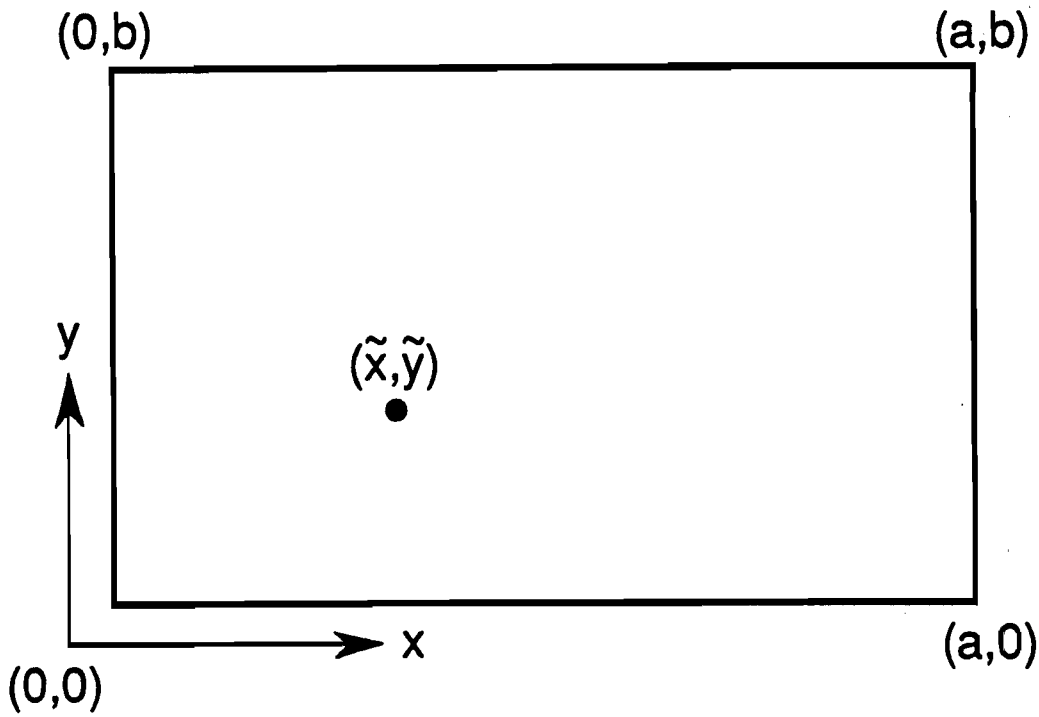

Figure 4. Simply Supported, Uniform Rectangular Plate with Damper Force at $(\tilde{x},\tilde{y})$.

Table: $A = ab = 1.0$ Meters Squared; $\tilde{x}/u = \tilde{y}/b = (1/\pi)$

a	r	$N \equiv a/b \equiv a^2$	$\delta_{ref} = .05$	$\delta_{ref} = .10$	$\delta_{ref} = .25$	$\delta_{ref} = .50$
.65	0.5529	.4225	1.7005	3.3506	8.7111	12.2702
.70	0.6372	.4900	1.7019	3.3618	8.7960	10.2591
.75	0.7307	.5625	1.7029	3.3696	8.9389	0.2759
.80	0.8316	.6400	0.0423	0.0834	0.1856	0.2574
.83	0.8937	.6889	0.0387	0.0743	0.1392	0.1346
.85	0.9345	.7225	0.0357	0.0616	0.0726	0.0379
.86	0.9572	.7396	0.0325	0.0469	0.0328	0.0071
.87	0.9785	.7569	0.0224	0.0193	0.0045	0.0052
.88	0.9998	.7744	0.0000	0.0000	0.0001	0.0002
.89	1.0211	.7921	0.0205	0.0196	0.0160	0.0170
.90	1.0423	.8100	0.0287	0.0401	0.0404	0.0406
.91	1.0635	.8281	0.0306	0.0500	0.0632	0.0658
.93	1.1058	.8649	0.0309	0.0564	0.0942	0.1170
.95	1.1478	.9025	0.0302	0.0572	0.1097	0.1437

Figure 5